Journal of
Applied Crystallography
ISSN 0021-8898

Received 16 August 2006
Accepted 15 January 2007

Small-angle neutron scattering from extended defects in diamonds

Andrei A. Shiryaev

Institute of Crystallography, RAS, Leninsky pr. 59, Moscow 119333, Russian Federation. Correspondence e-mail: shiryaev@ns.crys.ras.ru

The results of a small-angle neutron scattering investigation of natural and synthetic diamonds with variable concentrations and types of point defects and different degrees of deformation are reported. It is shown that deformation and/or annealing of diamonds lead to the formation of planar and three-dimensional defects, giving rise to small-angle scattering.

1. Introduction

The properties of diamonds depend strongly on the concentration and type of impurities and defects. Usually, defects are studied using a combination of spectroscopic techniques, such as infra-red (IR), visible and ultraviolet absorption, luminescence, and electron paramagnetic resonance (for comprehensive reviews, see Zaitsev, 2001; Field, 1992). This extensive body of work has led to a deep understanding of the most important points and of some extended defects. It has been established that nitrogen is the most important chemical impurity in synthetic and natural diamonds. IR absorption spectroscopy is the most widely used method to assess quantitatively the nitrogen concentration and principal N-containing defects. Common diamond classification is based on IR absorption spectra: diamonds with nitrogen impurities in different forms are termed type I (further subdivided to Ib and Ia, depending on predominant N-defects), and nitrogen-free diamonds (N concentration less than a few at.p.p.m.) are termed type II.

Whereas spectroscopic methods are suitable for the characterization of point defects, information about extended defects is less readily accessible. The properties of extended defects are usually addressed with transmission electron microscopy (TEM) and X-ray diffuse scattering in the vicinity of Bragg reflections. Besides defects common for other solids (dislocations, stacking faults *etc.*), diamonds contain platelets, which are very thin (2–3 interatomic spacings) planar defects with sizes reaching a few microns lying exclusively in the (100) plane and which consist of carbon interstitials and 10–20 at.% of nitrogen (Field, 1992; Fallon *et al.*, 1995). These platelets give rise to a sharp absorption peak in the IR spectrum and diffuse spikes around the 111 Bragg reflections. They have been extensively studied by TEM. Voidites, *i.e.* octahedral defects several nanometres in size, filled with low-density compounds, represent another important type of extended defect (Bruley & Brown, 1989; Kiflawi & Bruley, 2000). It is very important to note that platelets and voidites are related to the process of interconversion (so-called aggregation) of nitrogen point defects and appear only in crystals which have undergone special annealing.

However, despite numerous important achievements, the understanding of many point and extended defects is still insufficient. This statement is especially correct for optically inactive defects. Scattering and diffraction techniques, such as neutron and X-ray diffuse and small-angle scattering (SAS), are powerful methods for investigating extended defects in solids. Earlier, we reported the results of a small-angle X-ray scattering (SAXS) study of diamonds with variable concentration and type of nitrogen-related defects (Shiryaev *et al.*, 2000, 2001, 2003). It was shown that as-grown synthetic diamonds have a negligible SAXS intensity. However, subsequent high-temperature annealing leads to the appearance of scattering with variable intensity and angular distribution. Comparison of different as-received and annealed crystals led us to the conclusion that the scattering is caused by defects, for which the size decreases and the contrast with the diamond matrix increases with the degree of annealing. The appearance and intensity of the SAXS signal is not obviously related to the nitrogen content of the diamond. It should be noted that our previous work was performed using a linear detector. Although in many cases the SAXS patterns were recorded in several sample positions (samples were rotated), no clear indication of anisotropy was obtained and it was suggested that scattering defects are isometric. This paper extends the previous work and is devoted to the investigation of diamonds using small-angle neutron scattering. In particular, initial results for diamonds annealed and deformed at high pressures and temperatures are reported.

2. Experimental

Small-angle neutron scattering (SANS) measurements were performed on beamline D22 at ILL, Grenoble. The wavelength (λ) of the incident neutrons was 6 Å and the sample-to-detector distance was 8 m. Use of a two-dimensional detector allowed the study of the anisotropy of the scattering intensity. Samples were attached to a cadmium plate against a 2 mm hole. The SANS intensity was significant and in many cases a measurement time of 5 min was sufficient for a good quality pattern. Neutron absorption by the samples was low (transmission 96–97%). Experimental data were treated using *GRASP* software by (Dewhurst, 2003). Usually, the incident beam was directed along the [111] or [100] directions of the sample. Due to their complicated morphology, exact alignment of the natural diamonds studied was impossible, but the beam was directed roughly along the [111] and [110] directions. Where possible, the crystallographic orientation of the scattering defects was inferred from the orientation of the sample towards the incoming neutron beam and the angles between the spikes of the scattering patterns. The magnitude of the scattering vector is defined as $q = 4\pi\sin(\theta)/\lambda$ (Å^{-1}), where θ is half the scattering angle.

Prior to the scattering measurements, IR absorption spectra were acquired for all samples to obtain information about the nitrogen concentration and the type of N-related defects. The concentration was inferred using absorption by a diamond lattice as an internal standard and calibrations by Boyd *et al.* (1994) and Kiflawi *et al.* (1994). Spectra decomposition follows the procedure described by Bokii *et al.* (1986). A typical IR spectrum is shown in Fig. 1. Natural diamonds studied contain nitrogen impurities in concentrations ranging from ~0 to 1600 at.p.p.m. (~0–0.16 at.%). As is common for natural stones, nitrogen was present as A- and/or B-defects, *i.e.* as pairs of neighbouring substitutional atoms and 4 N complexes around a carbon vacancy, respectively. X-ray topography shows that the samples were plastically deformed to different extents.

Synthetic diamonds were represented by commercially produced polished [100]-oriented flats. Nitrogen in these stones was present as single substitutional atoms (C-defects, type Ib crystal) and its concentration was between 100 and 300 at.p.p.m., according to calibration by Kiflawi *et al.* (1994). The high crystalline quality of the synthetic diamonds in their as-received state was confirmed by X-ray topography.

High pressure–high temperature (HPHT) annealing of some of the synthetic samples was performed at 6.5 GPa and 1873 K in a multi-anvil apparatus. In several experiments, a special deformation cell which creates high deviatoric stresses and accompanying plastic deformation was used (Cordier & Rubie, 2001). In addition, different pressure-transmitting media were employed in order to mimic diamond deformation in nature. The microstructure of the samples was studied by several analytical methods and is described in Shiryaev *et al.* (2007). X-ray topographs and electron microscopy show a very high density of extended defects such as dislocations and twins in experimentally deformed diamonds. Note that, due to the extremely low diffusion coefficients of nitrogen and other impurities in diamond, annealing does not lead to any noticeable changes in the impurity content of the samples, but transformation of existing defects into other configurations may occur.

3. Results

Earlier, we attempted to correlate SAS patterns with the degree of nitrogen aggregation, which reflects the degree of diamond annealing. The intention to relate diamond characteristics to the nitrogen aggregation state is usually justified, since nitrogen-related defects determine mobility, charge state and other features of the majority of point defects. However, the current study shows that small-angle patterns are not so closely related to the nitrogen aggregation state; crystal microstructure plays an important role.

3.1. Nitrogen-free (type IIa) diamonds.

Two natural nitrogen-free (type IIa) diamonds were studied in this work. Despite virtually identical IR absorption spectra, the SANS patterns are drastically different. Whereas one of the samples shows featureless isotropic scattering, the other is totally different, having a cross-like pattern with lengthy spikes (Fig. 2). Interestingly, the diamonds came from the same geographic locality. This might indicate similar conditions of growth and subsequent annealing of the crystals in the Earth's mantle, although such an assumption should be taken with a certain amount of caution.

3.2. As-grown synthetic diamonds

Small-angle scattering from as-grown synthetic diamonds was virtually absent. This observation is in line with the results of our previous work (Shiryaev *et al.*, 2001, 2003), where no small-angle X-ray scattering was observed for such diamonds. Such behaviour is consistent with the suggestion that the nitrogen atoms are randomly distributed in the lattice.

3.3. Type I diamonds

Natural samples containing nitrogen in the A- and B-defects show some anisotropy in their SANS patterns. The patterns are sample-dependent (Fig. 3) and it is difficult to correlate the SANS data with the nitrogen concentration or speciation as inferred from IR measurements. Previous SAXS work on diamonds with intermediate degrees of nitrogen aggregation also showed strong variation from sample to sample. Scattering in these crystals is relatively weak and is due to polydisperse defects with broad size distributions. As is evident from the IR absorption spectra of the crystals studied, they contain extended defects termed platelets. However, in the SANS pattern, spikes corresponding to the planar precipitates in the (100) planes are weak and the presence of more isometric defects in addition to the platelets is highly likely. It should be noted that the rather irregular shape of the samples prevented a more detailed investigation of the scattering patterns as a function of their crystallographic orientation.

Two of the diamonds studied represent end members of the nitrogen aggregation process. They belong to the relatively rare IaB type of natural crystals containing high concentrations of nitrogen in

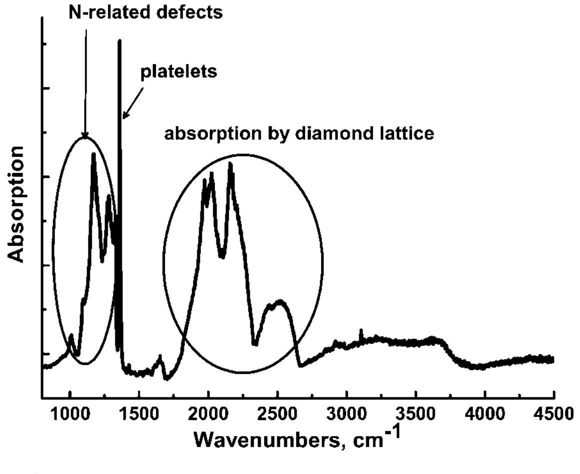

Figure 1
Typical IR absorption spectrum of diamond containing nitrogen in A- and B-defects as well as platelets.

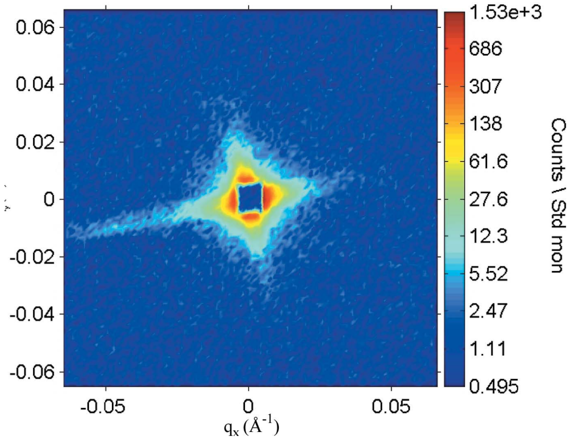

Figure 2
SANS pattern from type IIa (nitrogen-free) natural diamond.

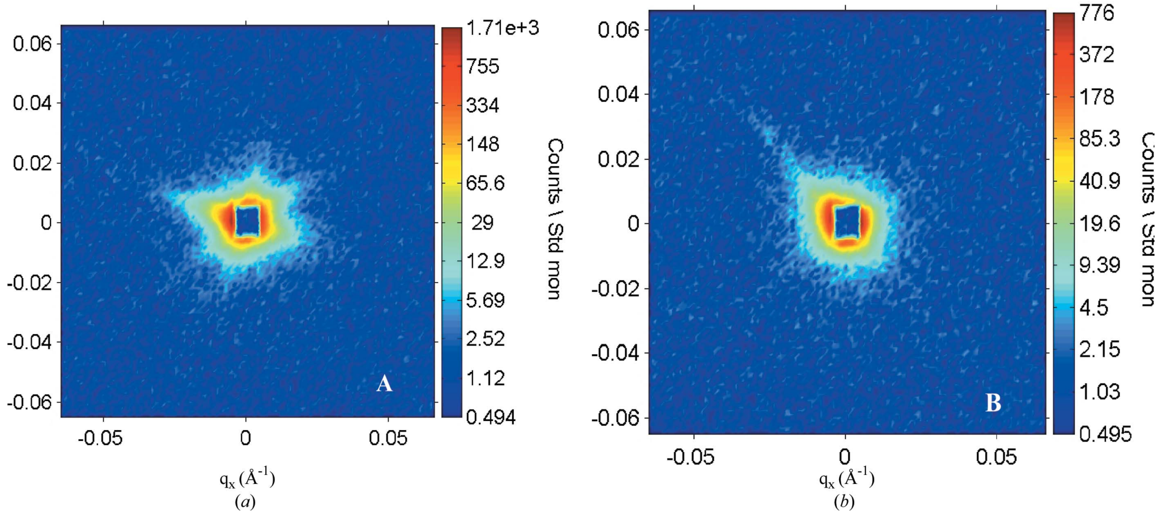

(*a*) (*b*)

Figure 3
SANS patterns from natural diamonds of type Ia. The samples contain a few hundred at.p.p.m. of nitrogen as the A- and B-defects, as well as platelets in the (100) plane. The sample in (*b*) contains nitrogen almost exclusively in the A-form. The IR spectrum of the sample shown in (*a*) is given in Fig. 1.

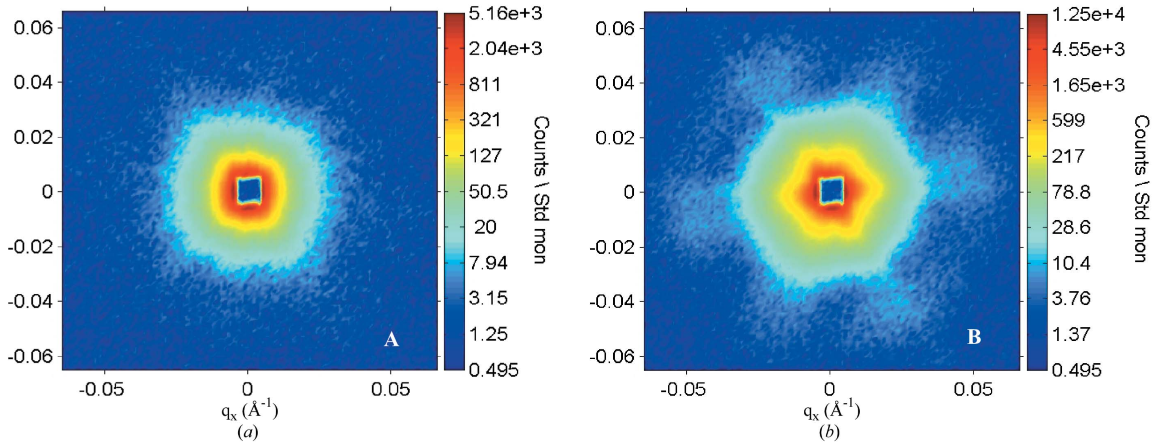

(*a*) (*b*)

Figure 4
Scattering from heavily annealed (type IaB) natural diamonds. The nitrogen concentration in the B-form is 400 and 580 at.p.p.m. for (*a*) and (*b*), respectively.

the form of B-defects only (4 N atoms around a vacancy) without platelets. It is known that in pure IaB type diamonds, the platelets undergo degradation to dislocation loops decorated by nanometre-sized defects called voidites (*e.g.* Bruley & Brown, 1989). An X-ray study showed the presence of a strong SAXS signal from type IaB diamonds caused by defects with a rather narrow size distribution around 8–9 nm (Shiryaev *et al.*, 2000). The current work shows that diamonds of this type are also strong neutron scatterers and the scattering patterns are sample-dependent. Whereas the scattering pattern from one of the diamonds is close to isometric (Fig. 4*a*), the second IaB sample demonstrates remarkable six-fold symmetry with possible Bragg-type peaks (Fig. 4*b*). The only difference between these two stones observed in their IR absorption spectra is that in one of the samples (Fig. 4*b*), the nitrogen concentration is slightly higher, *i.e.* 580 *versus* 400 at.p.p.m. However, it is doubtful that such a minor difference in the N concentration would account for the observed differences in the SANS patterns. Note that weak Bragg-like diffraction is observed in one of the IaB diamonds, indicating some ordering of the scatterers. At present we do not have a simple explanation of such periodicity. Understanding the scattering patterns from these two diamonds is complicated by differences in their morphology. The faces of one of the samples were slightly curved, which led to deviations from the selected crystallographic directions. This might have 'destroyed' the *n*-fold symmetry of the scattering pattern, as shown in Fig. 4*a*.

3.4. Deformed diamonds

In the current study, special attention was paid to the investigation of intentionally deformed diamonds. The microstructure of deformed diamonds depends strongly on the pressure-transmitting medium used in the deformation experiments. Deformation in the presence of numerous hard particles (such as SiC grains) introduces numerous dislocations (density up to 10^{12} cm^{-1}), whereas deformation in hard silicates leads to the creation of mechanical twins and stacking faults (Shiryaev *et al.*, 2007) and significantly fewer dislocations. It should be taken into account that all experimentally deformed diamonds are characterized by a relatively low nitrogen content (200–300 at.p.p.m.), mostly as single atoms with some fraction (up to 20%) of nitrogen pairs. The SANS patterns from the deformed diamonds are remarkably variable (Fig. 5), but one feature is common for all the samples, a marked anisotropy of the scattering intensity.

The shape of the scattering pattern and the intensity distribution depend strongly on the mechanical properties of the medium in

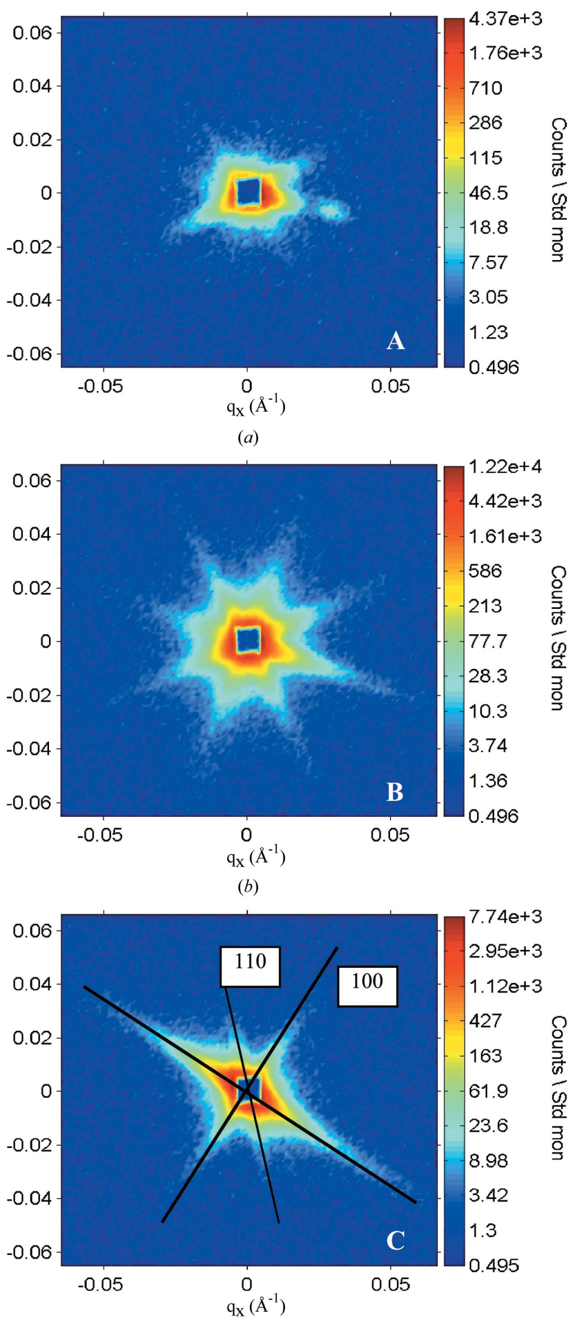

(*a*)

(*b*)

(*c*)

Figure 5
Scattering from experimentally deformed synthetic diamonds. The beam is along the [100] direction. The nitrogen concentration in the C-form is ~300 at.p.p.m. Deformation medium: (*a*) SiC grains, (*b*) hard silicates, (*c*) hard silicates and SiC grains.

contact with the diamond during annealing. Annealing in conditions favouring dislocation formation (in the presence of SiC grains) leads to the formation of a weakly anisotropic pattern, and up to eight spikes could be distinguished (Fig. 5*a*). Annealing in hard silicates results in the formation of mechanical twins and other similar imperfections (Fig. 5*b*), producing an eight-spike almost symmetric SANS pattern. The defects responsible for the scattering appear to be bounded by the (100) and (110) planes.

Finally, the SANS pattern of the diamond annealed in a mixture of hard silicates and SiC can be described as a superposition of a cross and one smaller diagonal, producing six spikes in total (Fig. 5*c*). From the SANS point of view, this sample qualitatively resembles one of the natural stones (Fig. 3*a*), although in the latter case the extent of the scattering intensity is smaller. Note, however, that the types of impurity-related defects in these two diamonds are very different. According to stereographic analysis, the defects are in the (100) and (110) planes, but in contrast with the case of diamond deformed in hard silicates, the scattering spikes are uneven. Most likely, this indicates that the conditions of the deformation strongly influence the crystallographic orientation of the defects.

4. Discussion

Several types of extended defects were found in diamonds during extensive TEM and X-ray investigations. Platelets in the (100) plane present in some natural diamonds are relatively well understood, but there is a growing body of evidence that planar defects in other crystallographic planes do exist. In an early SAXS study of low quality synthetic diamonds using photographic film, Woods (1970) observed spikes and ascribed them to scattering from thin (60–80 Å) films of metal alloys trapped during diamond growth and lying in the (111), (100), (113) and (110) planes. Since 1971, diamond growth technology has improved dramatically and modern crystals are of very high crystalline quality (*e.g.* Pal'yanov *et al.*, 1997). This is also reflected in the absence of SAS from modern as-grown synthetic diamonds. The presence of various planar and three-dimensional aggregates of impurities and intrinsic defects of unknown origin in natural diamonds was inferred from diffuse and small-angle X-ray scattering by various researchers (Lisoivan, 1978; Naletov *et al.*, 1977; Klyuev *et al.*, 1977; Ramanan *et al.*, 1998; Shiryaev *et al.*, 2003). However, to date no good explanation of the nature of the defects responsible for the X-ray patterns has been given.

Flat or faceted precipitates provide an explanation of the observed anisotropic SANS patterns. Transmission electron microscopy and X-ray topographic investigation of the deformed diamonds studied indicate the formation of stacking faults and mechanical twins and an increase in crystal mosaicity (Shiryaev *et al.*, 2007). Accompanying planar defects may, in principle, be responsible for the observed anisotropy of SANS, but it is not yet clear which of the above-mentioned defects may provide sufficient contrast. Scattering by planar defects is an attractive explanation, since it may explain the appearance of markedly uneven spikes in some of the observed patterns (*e.g.* Fig. 2). Slight rotation of the diamond crystal relative to the incident neutrons may lead to a loss of diffraction contrast.

Surprisingly, diamonds which certainly contain impurity-related (100) platelets show a relatively weak anisotropy of the SANS pattern (Fig. 3), although platelets give rise to strong diffuse X-ray scattering around the 111 Bragg reflections. This inconsistency might be explained by the fact that diffuse X-ray scattering by platelets is largely due to imposed stress fields, and only a small component, if any, is due to contrast in electron density. Fallon *et al.* (1995) suggested that platelets consist mostly of carbon with the addition of 10–20 at.% of nitrogen. If this observation is applicable to platelets in all diamonds, then the weakness of the neutron scattering might be due to a small contrast in nuclear density.

Some of the SANS patterns observed in the current study are likely due to three-dimensional (cuboid?) precipitates. Besides foreign inclusions, the only known three-dimensional defect is encountered in heavily annealed diamonds (type IaB), where voidites were observed by TEM and, possibly, by X-ray diffuse scattering (Lang *et al.*, 1985; Lisoivan, 1978; Naletov *et al.*, 1977). Voidites presumably contain nitrogen and hydrogen impurities (Bruley & Brown, 1989;

Kiflawi & Bruley, 2000) and should provide contrast for electron and neutron scattering. Scattering from such defects likely explains the SANS patterns of the type IaB diamonds studied.

The complexity of the observed SAS patterns and their sample-dependence indicate the simultaneous presence of different types of extended defects in natural and synthetic diamonds. Explanation of their origin requires the use of complementary methods of investigation such as X-ray and neutron scattering, electron microscopy *etc.* The same sample set was recently studied using two-dimensional SAXS and we are currently evaluating the results obtained. We hope that the comparison of neutron and X-ray datasets will provide a consistent explanation of the nature of the defects responsible for SAS. We are currently preparing a set of crystallographically oriented diamonds to facilitate the alignment of the crystal axes to the incoming beam.

5. Conclusions

The results of a SANS investigation of nitrogen impurities and with markedly different microstructures and different degrees of annealing are reported. It is shown that annealing and/or deformation lead to the appearance of a rather strong SANS signal. In many cases, considerable anisotropy of the scattering intensity distribution is present. In some of the diamonds, the existence of at least two types of scattering defects is plausible: (i) polydisperse particles giving isotropic scattering and (ii) anisotropic defects. Planar defects such as mechanical twins and impurity precipitates are among possible defects responsible for scattering in deformed diamonds. The contribution of three-dimensional defects such as voidites could be significant in some crystals. There is no clear relationship between nitrogen content and the features of the SAS patterns.

The help of D. J. Frost in the multianvil experiments and of F. Langenhorst in the TEM study is gratefully acknowledged. The support of R. P. May was essential in the data acquisition. Discussions with V. Volkov were very useful. Financial support from the Alexander von Humboldt Foundation and the Foundation for the Support of Russian Science is gratefully acknowledged. Comments by two anonymous reviewers were helpful.

References

Bokii, G.B., Bezrukov, G. N., Klyuev, Yu. A., Naletov, A. M. & Nepsha, V. I. (1986). *Natural and Synthetic Diamonds*. Moscow: Nauka. (In Russian).

Boyd, S. R., Kiflawi, I. & Woods, G. S. (1994). *Philos. Mag. B*, **69**, 1149–1153.

Bruley, J. & Brown, L. M. (1989). *Philos. Mag.* **59**, 247–261.

Cordier, P. & Rubie, D. C. (2001). *Mater. Sci. Eng. A*, **309–310**, 38–43.

Dewhurst, C. (2003). *GRASP*. http://www.ill.fr/lss/grasp

Fallon, A. J., Brown, L. M., Barry, J. C. & Bruley, J. (1995). *Philos. Mag. B*, **78**, 21–37.

Field, J. (1992). Editor. *The Properties of Natural and Synthetic Diamond*. London: Academic Press.

Kiflawi, I. & Bruley, J. (2000). *Diamond Relat. Mater.* **9**, 87–93.

Kiflawi, I., Mayer, A. M., Spear P. M., van Wyk, J. A. & Woods, G. S. (1994). *Philos. Mag. B*, **69**, 1141–1148.

Klyuev, Yu. A., Naletov, A. M., Nepsha, V. I., Epishina, N. I. & Buligina, T. A. (1977). *Sov. Phys. Solid State*, **19**, 7–10.

Lang, A. R., Kowalski, G., Makepeace, A. P. W. & Moore, M. (1985). *Philos. Mag.* **52**, L1–L6.

Lisoivan, V. I. (1978). *Sov. Phys. Dokl.* **21**, 469–471.

Naletov, A. M., Klyuev, Yu. A., Nepsha, V. I., Buligina, T. A. & Epishina, N. I. (1977). *Fiz. Tverdogo Tela*, **19**, 1529–1534. (In Russian)

Pal'yanov, Yu. N., Khokhryakov, A. F., Borzdov, Yu. M., Sokol, A. G., Gusev, V. A., Rylov, G. M. & Sobolev, N. V. (1997). *Russ. Geol. Geophys.* **38**, 882–885.

Ramanan, R. R., Goswami, S. N. N. & Lal, K. (1998). *Acta Cryst.* A**54**, 163–171.

Shiryaev, A. A., Dembo, K., Klyuev, Yu., Naletov, A. & Feigelson, B. (2003). *J. Appl. Cryst.* **36**, 420–424.

Shiryaev, A. A., Frost, D. J. & Langenhorst, F. (2007). *Diamond Relat. Mater.* In the press.

Shiryaev, A. A., Hutchison, M. T., Dembo, K. A., Dembo, A. T., Iakoubovskii, K., Klyuev, Yu. A. & Naletov, A. M. (2001). *Physica B*, **308–310**, 598–603.

Shiryaev, A. A., Klyuev, Yu. A., Naletov, A. M., Dembo, A. T. & Feigelson, B. N. (2000). *Diamond Relat. Mater.*, **9**, 1494–1499.

Woods, G. S. (1970). *Philos. Mag.* **22**, 1081–1084.

Zaitsev, A. M. (2001). *Optical Properties of Diamond: A Data Handbook*. Berlin: Springer-Verlag.